AD-A207 590 CRYSTAL AND MOLECULAR STRUCTURE OF TRIAMINOGUANIDINIUM 1/1
AZIDE (TAZ)(U) ARMY ARMAMENT RESEARCH DEVELOPMENT AND
ENGINEERING CENTER DOV.. A J BRACUTI MAY 89
UNCLASSIFIED ARAED-TR-88034 F/G 7/3 NL

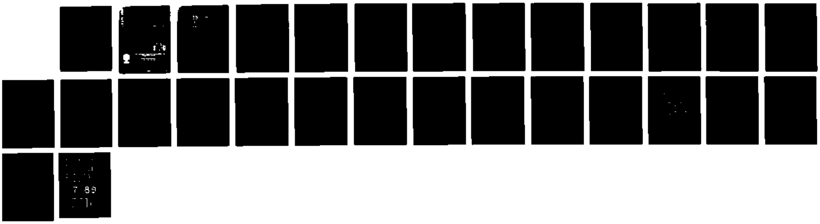

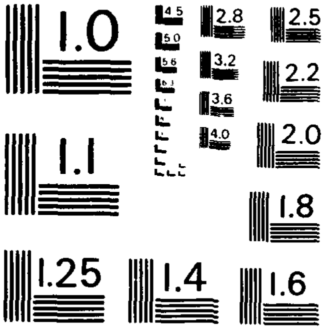
1.0
4.5
5.0
5.6
6.3
2.8
3.2
3.6
4.0
2.5
2.2
2.0
1.1
1.8
1.25
1.4
1.6

Technical Report ARAED-TR-88034

CRYSTAL AND MOLECULAR STRUCTURE OF TRIAMINOGUANIDINIUM AZIDE (TAZ)

A.J. Bracuti

May 1989

US ARMY
ARMAMENT MUNITIONS
& CHEMICAL COMMAND
ARMAMENT RDE CENTER

U.S. ARMY ARMAMENT RESEARCH, DEVELOPMENT AND ENGINEERING CENTER

Armament Engineering Directorate
Picatinny Arsenal, New Jersey

Approved for public release; distribution is unlimited.

UNCLASSIFIED
SECURITY CLASSIFICATION OF THIS PAGE

REPORT DOCUMENTATION PAGE

1a. REPORT SECURITY CLASSIFICATION UNCLASSIFIED

1b. RESTRICTIVE MARKINGS

2a. SECURITY CLASSIFICATION AUTHORITY

2b. DECLASSIFICATION/DOWNGRADING SCHEDULE

3. DISTRIBUTION/AVAILABILITY OF REPORT Approved for public release; distribution is unlimited.

4. PERFORMING ORGANIZATION REPORT NUMBER Technical Report ARAED-TR-88034

5. MONITORING ORGANIZATION REPORT NUMBER)

6a. NAME OF PERFORMING ORGANIZATION ARDEC, AED
Energetics and Warheads Div

6b. OFFICE SYMBOL SMCAR-AEE-BR

7a. NAME OF MONITORING ORGANIZATION

6c. ADDRESS (CITY, STATE, AND ZIP CODE) Picatinny Arsenal, NJ 07806-5000

7b. ADDRESS (CITY, STATE, AND ZIP CODE)

8a. NAME OF FUNDING/SPONSORING ORGANIZATION ARDEC, IMD
STINFO Br

8b. OFFICE SYMBOL SMCAR-IMI-I

9. PROCUREMENT INSTRUMENT IDENTIFICATION NUMBER

8c. ADDRESS (CITY, STATE, AND ZIP CODE) Picatinny Arsenal, NJ 07806-5000

10. SOURCE OF FUNDING NUMBERS

PROGRAM ELEMENT NO.	PROJECT NO.	TASK NO.	WORK UNIT ACCESSION NO.

11. TITLE (INCLUDE SECURITY CLASSIFICATION) CRYSTAL AND MOLECULAR STRUCTURE OF TRIAMINOGUANIDINIUM AZIDE (TAZ)

12. PERSONAL AUTHOR(S) A.J. Bracuti

13a. TYPE OF REPORT

13b. TIME COVERED FROM ________ TO ________

14. DATE OF REPORT (YEAR, MONTH, DAY) May 1989

15. PAGE COUNT 26

16. SUPPLEMENTARY NOTATION The Molecular Structure Corporation of College Station, TX, gathered the x-ray diffraction data

17. COSATI CODES

FIELD	GROUP	SUB-GROUP

18. SUBJECT TERMS (CONTINUE ON REVERSE IF NECESSARY AND IDENTIFY BY BLOCK NUMBER)
Molecular structure
Crystal structure
Triaminoguanidinium azide

19. ABSTRACT (CONTINUE ON REVERSE IF NECESSARY AND IDENTIFY BY BLOCK NUMBER)

A single-crystal structure determination of triaminoguanidinium azide was conducted. Lattice parameters, crystal structure, and molecular structure were determined.

20. DISTRIBUTION/AVAILABILITY OF ABSTRACT
☐ UNCLASSIFIED/UNLIMITED ☒ SAME AS RPT. ☐ DTIC USERS

21. ABSTRACT SECURITY CLASSIFICATION UNCLASSIFIED

22a. NAME OF RESPONSIBLE INDIVIDUAL I. HAZNEDARI

22b. TELEPHONE (INCLUDE AREA CODE) (201)724-3316

22c. OFFICE SYMBOL SMCAR-IMI-I

DD FORM 1473, 84 MAR

UNCLASSIFIED
SECURITY CLASSIFICATION OF THIS PAGE

CONTENTS

TABLES

FIGURES

INTRODUCTION

Triaminoguanidinium salts (TAGX) have been of interest to propellant formulators because of their propensity to accelerate the burning rates of cyclic nitramines such as RDX (ref 1). Also, because of their high nitrogen content, they have loomed on the propelling charge development horizon as the cool burning oxidizers of the future. One TAG salt in particular, which had captured the imagination of the formulator, was the azide (TAZ) because of its extremely high nitrogen content (87.5%). With this high nitrogen concentration, a low flame temperature is expected, as well as, a relatively high impetus, because copious volumes of gaseous decomposition products are also generated. At low pressures, according to Blake equilibrium code calculations, the theoretical decomposition products, are

$$CN_6H_9N_3 \rightarrow C + 9/2\ H_2 + 9/2\ N_2$$

But at higher pressures, this code predicts that carbon is consumed by its reacting with nitrogen and hydrogen to form also CH_4, NH_3, HCN and trace quantities of other compounds.

In a recent report (ref 2), it was shown that previous attempts by other to make trianminoguanidinium azide (TAZ) by two apparently straight forward aqueous methods yielded consistently bizarre results which were duplicated readily by this laboratory. As a result, previously attempted characterizations of the products formed by these methods were both inconsistent and unreliable. It was, therefore, concluded that those synethetic methods did not produce a single pure product and, at best, produced mixtures which contained some fraction of TAZ. To complicate matters, TAZ is apparently so very reactive in air, that initial small yields soon became infinitessimal. This set of circumstances guided this laboratory to attempt to synthesize TAZ by a totally different approach which would preclude both water and air from the reaction path and, in addition, would not rely on the formation of the unstable triaminoguanidine as a reaction intermediate. Since the utility of a nonaqueous cation exchange technique for making air-sensitive triaminoguanidine had been demonstrated previously (ref 3), a similar approach was prescribed for TAZ synthesis (ref 2). Another objective of that effort was to make enough pure TAZ to reliably characterize it.

This report describes in detail the crystal and molecular structure characterization of the TAZ product synthesized by the nonaqueous cation exchange technique developed by this laboratory.

EXPERIMENTAL

Data Collection

A pale pink acicular crystal of TAZ synthesized at ARDEC (ref 2) having approximate dimensions of 0.03 x 0.08 x 0.30 mm was mounted on a glass fiber in a random manner. The preliminary examination and data collection were performed with Mo Kα x-radiation (λ = 0.71073 A) on a Rigaku ASC5 computer-controlled diffractometer equipped with a graphite crystal incident-beam monochromator and a 12 kw rotating anode generator.

Cell constants and orientation matrix for data collection were obtained from least-squares refinement using the setting angles of 23 reflections in the angular range of $6<\theta<12$. As a check on crystal quality, omega scans of several intense reflections were measured. The width at reflection intensity half-height of each reflection was 0.25 with a take-off angle 6.0 which indicates good crystal quality.

The intensity data were collected at a temperatures of 23±1° C using the ω-θ technique with a scan rate of 24 deg/min (in omega). To assure good counting statistics, the intensities of weak reflections [$I<10\sigma(I)$] were measured by accumulating the counts from three successive rescans. Intensity data for 1841 reflections of which 1541 were unique and not systematically absent with h = 0 to 6, k = 0 to 7, and ℓ = -12 to 11 were collected to a maximum 2θ value of 40.0. The scan range (in deg) was determined as a function of θ to correct for the separation of the Kα doublet (ref 4). The scan width was calculated with the equation

$$\theta \text{ scan width} = 1.5 + 0.300 \tan\theta$$

The background level was determined by recording the counts at a fixed position on each side of the reflection. The ratio of peak counting-time to background countining-time was 2:1. The diameter of the incident beam collimator was 0.5 mm and the crystal-to-detector distance was 35 cm.

Data Reduction

Lorentz-polarization, but neither secondary extinction corrections (ref 5) nor absorption corrections, were applied to the intensity data. As a check on crystal and electronic stability, three representative reflections were measured every 41 min. No decay correction was applied to the reflection data-set because the intensities of these monitored reflections remained constant within experimental error throughout data collection. The agreement factor for the averaging of the 137 observed equivalent reflections was 3.2% based on intensity.

The crystal data are:

Monoclinic, space group $2_{1/c}$ (#14), a = 6.679 (2), b = 7.722 (2), c = 13.143 (4) A, β = 95.44 (2), V = 674.8 A^3, Z = 4, Dx = 1.45 g/cc, u = 1.2 cm^{-1}, F(000) = 312, Fw = 147.10, T = 296 K (23°C), systematic absences: $0k0$; $k = 2n + 1$; $h0\ell, \ell = 2n+1$.

On the basis of the sytematic absences

$0k0 \quad k = 2n+1$
$h0\ell \quad \ell = 2n+1$

and E probability distribution statistics the centrosymmetric space group $P2_1/c$ (#14) was selected.

Structure Determination

The positions of the nohydrogen atoms were found by direct methods (Enraf-nonius Structure Determination Package, ref 4) and the hydrogen atoms were located by difference Fourier techniques. The hydrogen atoms were refined with fixed isotropic thermal parameters while the nonhydrogen atoms were refined anisotropically by full-matrix least-squares in which the function $\Sigma w(|Fo| - |Fc|)^2$ was minimized and w is defined as $4Fo^2/\sigma(Fo)$. The standard deviation on intensities, $\sigma^2(Fo^2)$, is defined

$$\sigma^2(Fo^2) = [S^2 (C + R^2B) + (pFo^2)^2]/(Lp)^2$$

in which S is the scan rate, C is the total integrated peak count, B is the total background count, R is the ratio of the scan time to the background count, Lp is the Lorentz and polarization factor, and the parameter p is a factor introduced to down-weight the intense reflections. In this case p was set to 0.030.

The x-ray scattering factors were taken from Cromer and Waber (ref 6). Anomalous dispersion effects were included in the calculation of structure factors (ref 7) and the values of $\Delta f'$ and $\Delta f''$ were those of Cromer (ref 8). Only 341 reflections having intensities greater than 3.0 times their standard deviations were used in the refinement of the trial structure. The final cycle of refinement included 118 variables which converged (largest parameter shift was 0.01 times its esd) with an unweighted agreement factor of R = 0.037

$$R = \Sigma \, ||Fo| - |Fc||/\Sigma \, |Fo|,$$

and a weighted agreement factor of Rw = 0.038 in which

$$Rw = SQRT\ [\Sigma w\ (|Fo| - |Fc|)^2/\Sigma\ wFo^2]$$

The standard deviation of an observation of unit weight was 1.17. The highest peak in the final difference Fourier had a height of 0.27 e/A^3 with an estimated error based on F (ref 10) of 0.01.

DISCUSSION AND RESULTS

The atomic coordinates, thermal parameters, bond lengths, and bond angles of TAZ are presented in table 1 through table 4, respectively. Details of the hydrogen bonding are given in table 5, while molecular conformation data such as torsion angles and best least-squares-plane data are presented in tables 6 and 7, respectively. Both the TAG cation and azide anion are depicted in figure 1. The molecular structure of TAZ with hydrogen bonding represented by dashed lines and stereographic pairs of unit cells are presented in figures 2 and 3, respectively.

Description of the TAG Cation

The three C--N bonds (table 3) are equivalent with values of 1.334(8), 1.32(1), and 1.324(7) A. The three N--C--N angles are equivalent with values of 119.8(3), 120.39(3), and 119.9(4) which indicate a three-fold axis normal to the central carbon atom of the ionic plane. The N--N bonds are also equivalent with values of 1.408(9), 1.404(8), and 1.407(8) A. The average values for C--N and N--N are 1.326(8) and 1.406(8), respectively which agree with those in TAGN [C--N 1.322(6) and N--N 1.406(5) (ref 13)].

The conformation of the TAG cation presented in figure 1 displays C_3 symmetry which can be viewed as distorted C_{3h} symmetry somewhat reminiscent of the conformation reported for this cation in triaminoguanidinium 5-aminotetrazolate monohydrate (TAG 5AT) (ref 10) rather than strict C_{3h} symmetry which has been reported for this cation in triaminoguanidinium nitrate (TAGN) and triaminoguanidinium chloride (TAGC) (refs 11 and 12). With strict C_{3h} symmetry, all the nonhydrogen atoms and the imino hydrogen atoms would lie on the least-squares plane while amino hydrogen atom pairs would be bisected by this plane which in reality is a mirror plane normal to the three-fold axis. By contrast, with TAZ only, the nonhydrogen atoms are nearly planar which is demonstrated both by their torsion angles (table 6) which deviate only a few degrees from either 0 or 180 and by their relatively small deviations off the calculated least-squares plane (table 7). The imino hydrogen atoms, on the other hand, do not lie on the least-squares plane, and the amino hydrogen atom pairs while intersected by the least-squares plane are not strictly related by mirror symmetry. These deviations from C_{3h} symmetry probably are caused by the effects of hydrogen bonding.

Description of the Azide Anion

This triatomic anion depicted in figure 1 has two nonequivalent N--N bonds [N(7)--N(8) 1.188(7) and N(9)--N(8) 1.162(7) A, table 3] which are linear within experimental error [N(7)--N(8)--N(9) 179.2(7), table 4]. Usually, inorganic azide salts contain azide anions which have symmetric equivalent N--N bonds. The observed bond length difference in this salt, however, is probably the result of localized perturbation effects due to hydrogen bonding. The shorter N--N bond length agrees within experimental error with the N--N bond lengths found in ammonium azide (1.17(2) A, ref 14] while the longer bond length agrees with those found in potassium azide [1.184(1) A (ref 14)].

DESCRIPTION OF THE CRYSTAL STRUCTURE

This structure (figs. 2 and 3) consists of an infinite three-dimensional, hydrogen-bonded network of slightly puckered layers containing both the planar nonhydrogen atoms of TAG cations and the central nitrogen atoms of the linear triatomic azide anions. These layers nearly coplanar with (200) are held together by hydrogen bonding, van der Waals' and electrostatic forces. In general, each ion is surrounded by six oppositely charged ions; three of which are in the same layer, and three are in the adjacent layers. The nonplanar hydrogen atoms of each cation are also involved in hydrogen bonding between the two terminal nitrogen atoms of each linear azide anion which are located above and below the plane of the layer.

Each given layer is bonded to a set of neighboring layers which are not equidistant and, for convenience, are now defined as the near-layer and the far-layer. This results in an infinite array of parallel layers with alternating interionic separations in which each ion has three oppositely charged interlayer nearest-neighbors. Two hydrogen bonded nearest-neighbors are in the near-layer and one is in the far-layer. The distances for the hydrogen bonded anion-cation closest contacts with the near-layer are 3.140(8) [N(2)--H(3). . . N(9)] and 3.176(8) A [N(4)--H(6). . . N(9) and with the far-layer is 3.206(8) A [N(4)--H(5). . . N(7)]. The closest nonhydrogen bonded interlayer contact is 3.237(9) A [N(6)--N(7)].

The TAG cations are stacked approximately over each other in adjacent layers whose interlayer spacings alternate with closest far-layer cation contact for C--C of 3.25(1) and closest near-layer C--C contact of 3.45(1) A. On the surface, it seems contradictory to have closest cation-cation contact occurring between the far-layers rather than between the near-layers. This can be explained by looking down the a axis in figure 2, which reveals a slight zig-zagging of the stacked TAG cations in the projected bc plane. These lateral cation displacements have an effect on the carbon atom separations. Specifically, the lateral displacement of the TAG cation in the near-layer with respect to the reference TAG cation is greater than it is in the far-layer. Therefore, the cation-cation separation between adjacent layers with closest cation-anion contact (near-layers) is greater than it is between far-layers. The azide anions, on the other hand, are stacked over one another in alternate layers separated by 6.7A.

Only the amino hydrogen atoms of the TAG ion and terminal nitrogen atoms of the azide ion are involved in the interlayer hydrogen bonding network (table 5). The shorter interlayer hydrogen bonds of 3.140(8) A for N(2)--H(3) . . . N(9) with H . . . N distance of 2.39(7) A and a bond angle of 171(8) and 3.176(8) A for N(4)--H(6) . . . N(9) with H . . .N distance of 2.31 A and a bond angle of 158(6) bond the near layers, and the longest hydrogen bond of 3.206(8) A for N(4)--H(5) . . . N(7) with H . . . N distance of 2.19 A and a bond angle of 162 (5)] bonds the far layers.

A similar ionic arrangement occurs in TAGN (ref 11), but its higher symmetry produces a different layer packing scheme with repeating identical adjacent layer spacings rather than alternating ones.* The interlayer hydrogen bonded distance in TAGN is 3.103(5) (A) [with H . . . O of 2.22 A and bond angle of 178(4)], which is significantly closer than observed in TAZ.

Within each layer, each ion has three oppositely charged nearest neighbor ions. In addition to the coulombic forces, van der Wall's forces and hydrogen bonding operate within the layer. The hydrogen bonding, in this case, involves the interactions between the three imino hydrogen atoms of the TAG cation with the terminal nitrogen atoms of the azide anion. The shorter hydrogen bonded distances are equivalent with values of 3.010(8) and 3.017(δ*) A for N(1)--H(1) . . . N(7) and N(5)--H(7) . . . N(9), respectively and the longer hydrogen bonded distance is 3.106 A for N(3)--H(4) . . . N(7). This type of intralayer arrangement of ions is also present in TAGN, excpet in this case only two hydrogen bonds are formed but which are significantly shorter than those in TAZ. With TAGN, the first hydrogen bond is 2.849(5) A [H . . . O 1.98(5) and bond angle 160(5)] and the second is 2.880 (5) [H . . . O2.15(5) and bond angle 160(5)]. The closest within layer nonhydrogen bonded interionic contact between the TAG cation and the azide anion [N(3)---N(8)] is 3.280(8)A.

CONCLUSIONS

One would expect TAZ and TAGN to be isomorphic and to have similar ionic arrangements because it was previously reported that these two salts form substitutional solid solutions. It is somewhat surprising, however, to discover that TAZ displays monoclinic symmetry ($P2_1/c$) rather than orthorhombic symmetry (Pbcm) as does TAGN.

---

* To be accurate, the energetics and interatomic effects actually determine the symmetry displayed by the compound.

Despite the similarity between the two molecular structures, the TAZ structure is somewhat less tightly held together and as a result, TAZ is probably more readily affected by other reagents and external forces than is TAGN. This would help explain why TAZ crystals are more fragile and water soluble than TAGN; and why TAZ is hygroscopic and TAGN is not.

REFERENCES

1. Bracuti, A.J. and Picard, J.P., "TAG Nitrate Gun Propellant," Proceedings of the Third International Symposium, ARDEC, Picatinny Arsenal, New Jersey 07806-5000, October 1984.

2. Bracuti, A.J. and Manning, C.Y.," The Synthesis of Triaminoguanidinium Azide (TAZ)," Technical Report ARAED-TR-88015, ARDEC, Picatinny Arsenal, New Jersey, Aug 1988.5

3. Bracuti, A.J. and Manning, C.Y., "The Isolation of the Free Base on the Triaminoguanidinium Ion," Technical Report ARAED-TR-87019, Picatinny Arsenal, New Jersey, June 1987.

4. Frenz, B.A., "Computing Crystallography," edited by Shrenk, M.; Olthof-Hazelkamp, T.; van Konigsveld, H.; and Bassi, G.C., Delft University, Delft Holland, 1978.

5. Zacharaiasen, W.H., "The Secondary Extinction Correction," Acta Cryst., 16, pp 1139-1144, 1963.

6. Cromer, D.T. and Waber, J.T., International Tables for X-Ray Crystallography, Vol IV, p 99, The Kynoch Press, Birmingham, England, 1974 (present distributor D. Riedel, Dordrecht).

7. Ibers, J.A. and Hamilton, W.C., "Dispersion Corrections and Crystal Structure Refinements," Acta Cryst., 17, p 781, 1964.

8. Cromer, D.T., International Tables for X-Ray Crystallography, Vol IV, pp 149-150, The Kynoch Press, Birmingham, England, 1974 (present distributor D. Riedel, Dordrecht).

9. Cruickshank, D.W.J., "The Accuracy of Atomic Coordinates Derived by Least-Squares or Fourier Methods," Acta Crystal, 2, p 154, 1949.

10. Bracuti, A.J. Troup, J.M., "An Examination of the Structural Features of Triaminoguanidinium 5-Aminotetrazolate Monohydrate," Technical Report ARAED-TR-86049, ARDEC, Picatinny Arsenal, New Jersey, March 1987.

11. Bracuti, A.J., "The Crystal Structure Determination of Triaminoguanidinium Nitrate: A Burning Rate Modifier for Nitramine Propellants," Technical Report ARLCD-TR-78050, ARRADCOM, Dover, New Jersey, February 1979.

12. Bracuti, A.J., "The Crystal Structure of Triaminoguanidinium Chloride," Acta Cryst., C39, pp 1465-1467, 1983.

13. Choi, C.S., "Energetic Materials," Vol 1, pp 100-101, edited by H.D. Fair and R.F. Walker, Plenum Press, New York and London, 1977.

14. Bracuti, A.J., "Triaminoguanidinium Azide Nitrate (TAZN)," Technical Report ARAED-TR-87017, ARDEC, Picatinny Arsenal, New Jersey, June 1987.

Table 1. Atomic coordinates

Atom	X	Y	Z
C(1)	0.743(1)	0.513(1)	0.0032(7)
N(1)	0.7175(8)	0.6121(8)	-0.0803(5)
N(2)	0.638(1)	0.791(1)	-0.0659(5)
N(3)	0.740(1)	0.5846(7)	0.0945(5)
N(4)	0.758(1)	0.4747(9)	0.1800(5)
N(5)	0.7760(9)	0.3452(7)	-0.0060(4)
N(6)	0.7749(9)	0.2768(8)	0.1053(5)
H(1)	0.710(9)	0.557(8)	-0.143(5)
H(2)	0.56(1)	0.820(8)	-0.107(5)
H(3)	0.77(1)	0.83(1)	-0.087(6)
H(4)	0.72(1)	0.681(9)	0.096(6)
H(5)	0.62(1)	0.480(8)	0.210(5)
H(6)	0.86(1)	0.521(8)	0.223(5)
H(7)	0.80(1)	0.280(9)	0.48(5)
H(8)	0.66(1)	0.199(8)	-0.121(5)
H(9)	0.88(1)	0.213(9)	-0.106(5)
N(7)	0.625(1)	-0.672(8)	0.1920(4)
N(8)	0.773(1)	-0.0072(7)	0.1629(4)
N(9)	0.917(1)	0.0512(8)	0.1333(5)

Table 2. General anisotropic temperature factors and their estimated standard deviations

	U11	U22	U33	U12	U13	U23
	0.025(4)	0.034(5)	0.029(5)	-0.003(4)	0.004(4)	0.002(5)
N(1)	0.052(4)	0.030(5)	0.034(4)	0.004(3)	0.003(3)	-0.004(4)
N(2)	0.055(5)	0.038(5)	0.055(4)	0.002(4)	0.009(3)	0.009(3)
N(3)	0.051(4)	0.039(5)	0.027(4)	-0.001(4)	0.000(3)	-0.001(4)
N(4)	0.044(5)	0.066(5)	0.024(4)	0.003(4)	0.003(3)	0.003(3)
N(5)	0.056(4)	0.029(5)	0.031(5)	0.004(3)	0.009(3)	-0.001(3)
N(6)	0.047(4)	0.048(4)	0.046(4)	0.008(4)	0.002(4)	-0.023(4)
N(7)	0.043(4)	0.063(5)	0.038(4)	0.001(4)	0.015(3)	0.002(3)
N(8)	0.052(5)	0.021(4)	0.023(4)	0.013(4)	0.003(4)	0.001(3)
N(9)	0.055(4)	0.053(5)	0.056(5)	-0.006(4)	0.013(4)	0.009(4)
H(1)	0.054					
H(2)	0.065					
H(3)	0.065					
H(4)	0.053					
H(5)	0.061					
H(6)	0.053					
H(7)	0.058					
H(8)	0.061					
H(9)	0.061					

Table 3. Bond lengths and their estimated standard deviations

Atom 1	Atom 2	Distance
C(1)	N(1)	1.334(8)
C(1)	N(3)	1.32(1)
C(1)	N(5)	1.324(7)
N(1)	N(2)	1.408(9)
N(1)	H(1)	0.92(6)
N(2)	H(2)	0.97(6)
N(2)	H(3)	0.76(7)
N(3)	N(4)	1.404(8)
N(3)	H(4)	0.75(7)
N(4)	H(5)	1.05(6)
N(4)	H(6)	0.91(6)
N(5)	N(6)	1.407(8)
N(5)	H(7)	0.86(6)
N(6)	H(8)	0.97(6)
N(6)	H(9)	0.84(6)
N(7)	N(8)	1.188(7)
N(8)	N(9)	1.162(7)

Table 4. Bond angles and their estimated standard deviations

Atom 1	Atom 2	Atom 3	Angle (deg)
N(1)	C(1)	N(3)	119.8(3)
N(1)	C(1)	N(5)	120.3(3)
N(3)	C(1)	N(5)	119.9(4)
N(2)	N(1)	C(1)	118.9(3)
N(4)	N(3)	C(1)	117.4(3)
N(6)	N(5)	C(1)	118.5(3)
N(2)	N(1)	H(1)	112.0(3)
N(4)	N(3)	H(4)	124.0(3)
N(6)	N(5)	H(7)	112.0(2)
C(1)	N(1)	H(1)	118.0(4)
C(1)	N(3)	AH(4)	117.0(6)
C(1)	N(5)	H(7)	121.0(5)
N(1)	N(2)	H(2)	108.0(4)
N(1)	N(2)	H(3)	104.0(6)
N(2)	N(1)	H(1)	125.0(6)
N(3)	N(4)	H(5)	105.0(4)
N(3)	N(4)	H(6)	105.0(4)
N(4)	N(3)	H(4)	125.0(6)
N(5)	N(6)	H(8)	112.0(4)
N(5)	N(6)	H(9)	107.0(5)
N(6)	N(5)	H(7)	121.0(5)
H(2)	N(2)	H(3)	110.0(7)
H(5)	N(4)	H(6)	113.0(6)
H(8)	N(6)	H(9)	104.0(6)
N(7)	N(8)	N(9)	179.2(7)

Table 5. Details of hydrogen bonds between donor (D) and acceptor (A) atoms and their estimated standard deviations

D( )--H( ) . . . ( )	D . . . A	H . . . A	D-H . . . . A
N(1)--H(1) . . . N(7)	3.017(8)	2.20(6)	149(8)
N(3)--H(4) . . . N(7)	3.106(8)	2.44(7)	149(8)
N(4)--H(5) . . . N(7)	3.206(8)	2.19(7)	162(5)
N(5)--H(7) . . . N(9)	3.010(8)	2.21(7)	154(6)
N(2)--H(3) . . . N(9)	3.140(9)	2.39(7)	171(8)
N(4)--H(6) . . . N(9)	3.176(8)	2.31(7)	158(6)

Table 6. Torsion angles and their estimated standard deviation

Atom					Atom				
(1)	(2)	(3)	(4)	Angle (deg)	(1)	(2)	(3)	(4)	Angle (deg)
N(1)	C(1)	N(3)	H(4)	1(6)	C(1)	N(3)	N(4)	H(6)	128(4)
N(1)	C(1)	N(3)	N(4)	177.0(6)	C(1)	N(3)	N(4)	H(5)	-113|(4)
N(1)	C(1)	N(5)	H(7)	178(5)	C(1)	N(5)	N(6)	H(9)	133(5)
N(1)	C(10	N(5)	N(6)	-2(1)	C(1)	N(5)	N(6)	H(8)	-113(4)
N(2)	N(1)	C(1)	N(3)	-1(1)	C(1)	N(1)	N(2)	H(3)	118(6)
N(2)	N(1)	C(1)	N(5)	-180(2)	C(1)	N(1)	N(2)	H(2)	-125(4)
N(3)	C(1)	N(5)	H(7)	-1(6)	H(2)	N(2)	N(1)	H(1)	48(6)
N(3)	C(1)	N(5)	N(6)	179.0(5)	H(5)	N(4)	N(3)	H(4)	63(8)
N(3)	C(1)	N(1)	H(1)	-175(4)	H(9)	N(6)	N(5)	H(7)	-47(7)
N(4)	N(3)	C(1)	N(5)	-4(1)	H(1)	N(1)	N(2)	H(3)	-69(8)
N(5)	C(1)	N(3)	H(4)	179(6)	H(4)	N(3)	N(4)	H(6)	-56(8)
N(5)	C(1)	N(1)	H(1)	6(4)	H(7)	N(5)	N(6)	H(8)	66(7)

Table 7. Least squares plane for TAZ cation

Atoms defining plane	Distance from plane, A
C	0.008(6)
N(1)	0.002(6)
N(2)	0.011(7)
N(3)	0.027(6)
N(4)	-0.032(6)
N(5)	0.021(6)
N(6)	-0.021(6)
Off-plane atoms	
H(1)	-0.08
H(2)	-0.77
H(3)	0.63
H(4)	0.03
H(5)	-0.96
H(6)	0.68
H(7)	0.05
H(8)	-0.84
H(9)	0.57

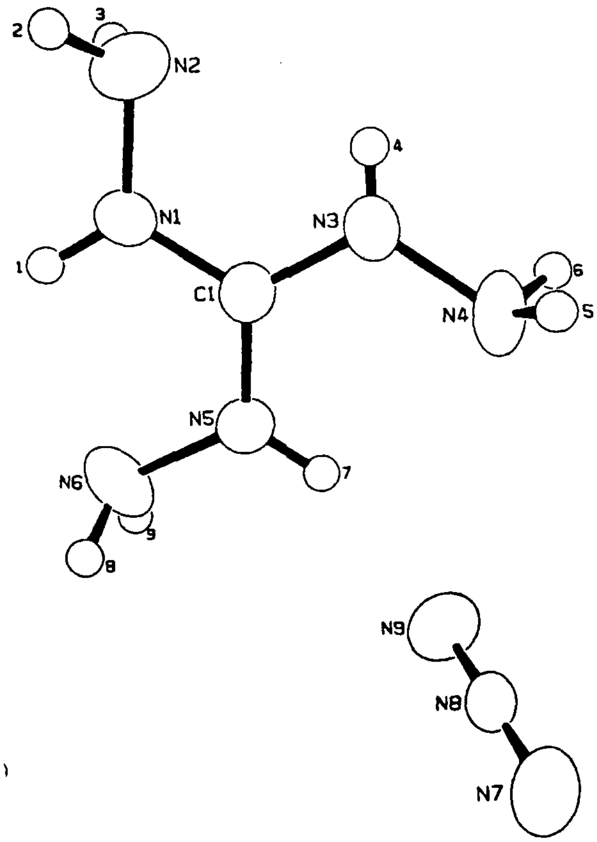

Figure 1. Triaminoguanidinium azide. (Ortep plot with heavy atom thermal ellipsoids scaled to enclose 50% probability and hydrogen atoms arbitrarily scaled for visual clarity.)

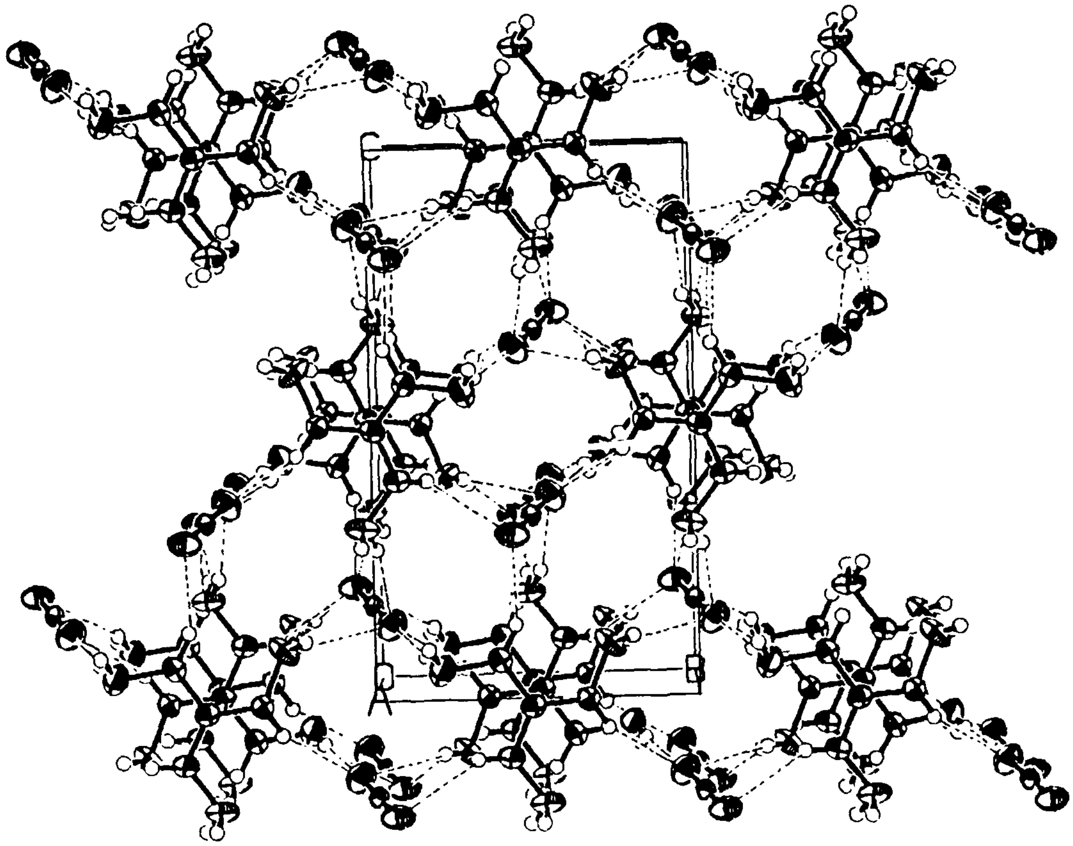

Figure 2. Triaminoguanidinium azide unit cell viewed down the a axis. (Hydrogen bonds depicted by dashed lines, Ortep plot with heavy atom thermal ellopsoids scaled to enclose 50% probability and hydrogen atom thermal ellipsoids arbitrarily scaled for visual clarity.

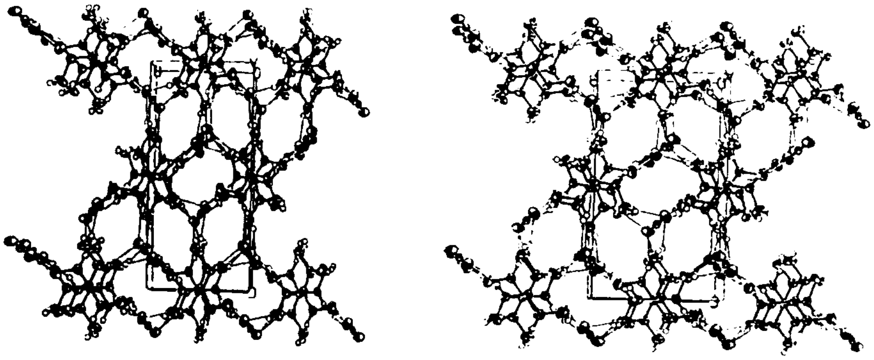

Figure 3. Stereo pair of unit cells containing triaminoguanidinium azide viewed down the a axis. (Hydrogen bonds depicted by dashed lines; Ortep plot with heavy atoms thermal ellipsoids scaled to enclose 50% probability; hydrogen atom thermal ellipsoids scaled arbitrarily for visual clarity.

DISTRIBUTION LIST

Commander
Armament Research, Development and Engineering Center
U.S. Army Armament, Munitions and Chemical Command
ATTN: SMCAR-IMI-I (5)
SMCAR-AEE (4)
SMCAR-AEE-BR, A. Bracuti (10)
C.Y. Manning
Picatinny Arsenal, NJ 07806-5000

Commander
U.S. Army Armament, Munitions and Chemical Command
ATTN: AMSMC-GCL(D)
Picatinny Arsenal, NJ 07806-5000

Administrator
Defense Technical Information Center
ATTN: Accessions Division (12)
Cameron Station
Alexandria, VA 22304-6145

Director
U.S. Army Materiel Systems Analysis Activity
ATTN: AMXSY-MP
Aberdeen Proving Ground, MD 21005-5066

Commander
Chemical Research, Development and Engineering Center
U.S. Army Armament, Munitions and Chemical Command
ATTN: SMCCR-MSI
Aberdeen Proving Ground, MD 21010-5423

Commander
Chemical Research, Development and Engineering Center
U.S. Army Armament, Munitions and Chemical Command
ATTN: SMCCR-RSP-A
Aberdeen Proving Ground, MD 21010-5423

Director
Ballistic Research Laboratory
ATTN: AMXBR-OD-ST, J. Frasier
J. Rocchio
I. May
I. Stabie
C. Knapton
Aberdeen Proving Ground, MD 21005-5066

Chief
Benet Weapons Laboratory, CCAC
Armament Research, Development and Engineering Center
U.S. Army Armament, Munitions and Chemical Command
ATTN: SMCAR-CCB-TL
Watervliet, NY 12189-5000

Commander
U.S. Army Armament, Munitions and Chemical Command
ATTN: SMCAR-ESP-L
Rock Island, IL 61299-6000

Director
U.S. Army TRADOC Systems Analysis Activity
ATTN: ATAA-SL
White Sands Missile Range, NM 88001

Director of Army Research and Technology
ATTN: DAMA-AR, L.M. Cameron
Pentagon Room 3E474
Washington, DC 20310

Director
LABCOM
Harry Diamond Laboratory
2800 Powder Mill Road
Adelphia, MD 20783-1145